JAAS

ROYAL SOCIETY OF CHEMISTRY

PAPER

View Article Online
View Journal | View Issue

Check for updates

Cite this: *J. Anal. At. Spectrom.*, 2023, **38**, 939

A two-stage Cd purification method with anion exchange resin and BPHA extraction resin for high precision determination of Cd isotopic compositions by double spike MC-ICP-MS

Qiao-Hui Zhong,[abc] Jie Li, *[ab] Lu Yin,[d] Neng-Ping Shen,[e] Shuang Yan,[bf] Zhao-Yang Wang[abc] and Chun-Hui Zhu[g]

TRU Spec resin is commonly used to purify Cd from residual Sn, however, this resin can induce anomalous interference on Cd isotopic measurement which may be attributed to phosphor bound organics that are eluted along with Cd fractions. In this study, progressive $\delta^{114/110}Cd_{NIST\ 3108}$ isotopic positive shifts are observed with the increase of the concentration ratio of [P/Cd] (*e.g.*, ≥100), which further confirms the interference of P on Cd isotopic measurement. Furthermore, mass scans of the P solution reveals no interfering ion beams across the Cd mass range (masses 106 to 116). These results indicate that anomalous shifts in the Cd isotope measurement may be caused by P-related matrix effects. Here, BPHA extraction resin instead of TRU Spec resin is employed to further purify Cd from residual Sn after the separation of Cd using an anion exchange resin column (AG-MP-1M). The BPHA extraction resin is made of *N*-benzoyl-*N*-phenylhydroxylamine (BPHA) impregnation into a microporous acrylic ester polymeric resin (CG-71) without phosphorous organic compounds. This resin exhibits a good ability to purify Cd fractions from interference elements such as Sn, Mo, Zr, and Nb. Cd isotope ratios are determined using double spike MC-ICP-MS. The $\delta^{114/110}Cd_{NIST\ 3108}$ values of geological reference materials determined by the presented method are in agreement with previous results within analytical uncertainties. The results confirm that our proposed method is suitable for accurate and precise determination of Cd isotopic compositions in low-Cd geological samples.

Received 11th December 2022
Accepted 15th February 2023

DOI: 10.1039/d2ja00411a

rsc.li/jaas

1. Introduction

Cadmium (Cd), a chalcophile element, consists of eight stable isotopes including ^{106}Cd (1.25%), ^{108}Cd (0.89%), ^{110}Cd (12.47%), ^{111}Cd (12.80%), ^{112}Cd (24.11%), ^{113}Cd (12.23%), ^{114}Cd (28.74%) and ^{116}Cd (7.52%).[1] The interest in the wide application of Cd stable isotopic systems has increased significantly in recent decades. Cadmium isotopes can be employed to study the evolution of the cosmochemistry system,[2,3] and investigate the formation processes of Pb–Zn ore deposits.[4–7] Additionally, Cd isotopes are broadly utilized to study the biological cycling of Cd in the marine environment,[8–13] to reconstruct the Cd isotopic composition of seawater,[14,15] and levels of primary productivity of paleoceanography.[16–18] With the increasing Cd pollution problems, the sources and fates of Cd in surface environments are traced with Cd isotopic fingerprint information.[19–28]

Cd isotopic ratios were first measured by TIMS obtaining an external precision for $\delta^{114/110}$Cd of 3.2–6.4‰ (2SD), which cannot distinguish Cd isotopic fractionation in most geological/environmental samples from the experimental standard.[29] Thanks to the advent of MC-ICP-MS, high-precision Cd isotope measurement was first carried out by Wombacher *et al.* (2003).[2] With further advances in instruments (both MC-ICP-MS and TIMS), more high-precision analysis of Cd isotopes was achieved and reported.[30–37] Cadmium isotopes are reported in the delta (δ) notation in per mil deviation (‰) relative to NIST SRM 3108 using the formula: $\delta^{114/110}Cd = ((^{114}Cd/^{110}Cd)_{sample}/(^{114}Cd/^{110}Cd)_{NIST\ SRM\ 3108} - 1) \times 1000$.

The purification of Cd from matrix elements is the prerequisite for obtaining high-precision Cd isotopic data. Chromatography employing anion exchange resin (AG1-X8 or AG-MP-1M) is commonly used for Cd purification from geological,

[a]*State Key Laboratory of Isotope Geochemistry, Guangzhou Institute of Geochemistry, Chinese Academy of Sciences, Guangzhou, 510640, China. E-mail: jieli@gig.ac.cn*
[b]*CAS Center for Excellence in Deep Earth Science, Guangzhou, 510640, China*
[c]*College of Earth and Planetary Sciences, University of Chinese Academy of Sciences, Beijing, 100101, China*
[d]*Hebei Key Laboratory of Strategic Critical Mineral Resources, Hebei GEO University, Shijiazhuang, 050031, China*
[e]*State Key Laboratory of Ore Deposit Geochemistry, Institute of Geochemistry, Chinese Academy of Sciences, Guiyang, 550081, China*
[f]*CAS Key Laboratory of Mineralogy and Metallogeny, Guangzhou Institute of Geochemistry, Chinese Academy of Sciences, Guangzhou 510640, Guangdong, China*
[g]*Tongwei Analytical Technology Co., Ltd, Guangzhou 510640, China*

biological, and environmental materials. In general, these column procedures can be grouped into two main types. A single-column procedure with AG-MP-1M anion exchange resin was first proposed by Cloquet *et al.* (2005)[30] utilizing various concentrations of HCl to remove matrix elements and separate Cd from environmental samples. This simple procedure then has been widely followed and further modified by many studies for separating Cd from different sample types.[4,33,34,36–39] However, Cd cannot be completely separated from Sn with only a one-column procedure with AG-MP-1M anion exchange resin.[30,34,36–39] Besides Sn, Mo may also be potentially eluted into Cd in some samples with high Mo contents.[36,39] However, Sn and Mo, as important interfering ions on Cd isotopic measurement, generally have a much larger content than Cd in most geological samples. For solving the residual Sn and potential Mo in Cd, a two-column procedure with AG-MP-1M anion exchange resin was proposed, which took a long column running time.[36]

Additionally, a two-column procedure with AG1-X8 anion exchange resin and TRU Spec resin (Eichrom, USA) was first developed by Wombacher *et al.* (2003)[2] for separating Cd from geological samples. The AG1-X8 anion exchange resin column could remove the most matrix element, and then the TRU Spec resin column was further utilized to separate Cd from residual Sn. This method is then adopted and improved by many studies for different samples (*e.g.*, seawater, plant, soil, rock, meteorite, and carbonates).[15,31,32,35,40–42] However, TRU Spec resin-derived organics can also be eluted alongside Cd from the TRU Spec resin column, which can then induce very anomalous Cd isotopic results even with a reliably double spike for the correction of instrumental mass fractionation.[41,43] Gault-Ringold and Stirling (2012)[43] concluded that the inaccurate results stemmed from the resin-derived residual organics, which were caused by one or more polyatomic interferents or anomalous mass bias behavior (*e.g.*, mass-independent or non-exponential mass-dependent isotope fractionation). Murphy *et al.* (2015)[41] speculated that the presence of TRU resin-derived organic compounds which were generated by partial oxidation may change the distribution of isotopes in the plasma and thus alter both the extent and mass dependence of the instrumental mass bias. But the real reason for Cd isotopic anomalies related to TRU resin-derived organic compounds remains unclear.

To separate pure Cd from low-Cd geological samples for precise and accurate Cd isotopic determination, we present a new analytical protocol for Cd purification. Here, BPHA extraction resin is utilized for further Cd separation from interference element Sn. Besides Sn, BPHA extraction resin also exhibits highly selective adsorption for the interference elements Mo, Zr, and Nb. Based on the purification using AG-MP-1M anion exchange resin (100–200 mesh) and BPHA extraction resin columns, interference elements, especially In, Ga, Ge, Zn, Sn, Mo, Zr, and Nb can be effectively and quantitatively separated from Cd fractions. The double spike method is employed to correct potential Cd isotopic fractionation during Cd chemical separation and instrument bias during MC-ICP-MS measurements.

2. Experimental procedure

2.1 Reagents and samples

HF (BVIII grade reagent, Beijing Institute of Chemical Reagents, China) is purified once using a Savillex DST-1000 sub-boiling acid system (Savillex, Eden Prairie, Minnesota, USA), and HCl/HNO_3 (BVIII electronic grade, Beijing Institute of Chemical Reagents, China) is purified twice. Ultra-pure water (Milli-Q H_2O, 18.2 MΩ cm) is generated from a Milli-Q system (Millipore). The Savillex™ PFA (7, 15, and 22 mL) beakers are sequentially cleaned with 1 : 1 (v/v) HNO_3, 1 : 1 (v/v) HCl, and Milli-Q H_2O before use. Two different Teflon columns of 15 cm × 6 mm i.d. and 6 cm × 5 mm i.d., are utilized for purification work in the first and second columns, respectively. Additionally, other materials such as columns, pipette tips, and tubes are sequentially washed in a heated bath (60 °C) of 2% HNO_3 (v/v) and Milli-Q H_2O before use. The AG-MP-1M anion exchange resin (100–200 mesh) is bought from Bio-Rad Company, USA. The theoretical capacity of AG-MP-1M anion exchange resin is 1 meq mL^{-1}, which gives a mass equivalent for Cd of 56.2 mg mL^{-1}.[44,45] *N*-Benzoyl-*N*-phenylhydroxylamine(BPHA) resin is commercially unavailable and prepared by following the procedures described by Li *et al.* (2014).[46] The spikes ^{111}Cd and ^{113}Cd are purchased from the Oak Ridge National Laboratory, USA. ICP-MS standard solutions (1000 μg mL^{-1}) of P, Zr, Cd, Mo, Nb, and Sn are purchased from Beijing General Research Institute for Nonferrous Metals (BGRINM, China).

Three pure Cd standard solutions including NIST SRM 3108, BAM I012 Cd, and Spex Cd are used here. NIST SRM 3108 is purchased from the National Institute of Standards and Technology (NIST), USA. BAM I012 Cd and Spex Cd are generously provided by Dr Zhu at the China University of Geosciences (Beijing). The BAM-I012 (Lot: C152382M, 1000 μg mL^{-1}) and Spex-Cd (Lot: CL8-71CDY, 1000 μg mL^{-1}) were purchased from the German Bundesanstalt für Material forschung und-prüfung (BAM) and Merck (China), respectively.[36] Reference materials of ferromanganese nodules (NOD-P-1 and NOD-A-1) and rock (COQ-1, BCR-2, BHVO-2, AGV-2, and GSP-2) are bought from the US Geological Survey (USGS).

2.2 Sample digestion

Approximately 25–500 mg of sample powder containing 30–100 ng Cd (typical 30 ng) is weighed accurately into a Teflon sample bomb, and 2–3 drops of Milli-Q H_2O are added to wet the samples. According to the concentration ratio of Cd_{spike} : Cd_{sample} = 1 : 1, suitable Cd spike solutions are weighed accurately into the Teflon sample bombs to avoid Cd isotopic fractionation during sample dissolution and chemical purification. 0.75 mL concentrated HNO_3 (15.5 mol L^{-1}) and 2.25 mL HF (25.4 mol L^{-1}) are added sequentially, and then the Teflon sample bombs are sealed and then placed into an oven at 190 °C for 72 h to break down and dissolve the solid minerals as well as organic materials completely. After that, samples are transferred into Savillex™ PFA beakers and evaporated to dryness. To completely dissolve the samples, suitable aqua regia (HCl : HNO_3 = 3 : 1, v/v) is added to the Savillex™ PFA beakers on

a hotplate, at 130 °C overnight. After evaporating the samples again, 3 mL 6 M HCl is added into the Savillex™ PFA beakers to decompose residual solids completely. This procedure is repeated. Finally, the samples are redissolved in 2 mL 2 M HCl for further chemical separation.

2.3 Cadmium isotopic purification

All experiments were conducted in Tongwei Analytical Technology Co., Ltd (Guiyang). The two-column protocol is outlined in Table 1 and is briefly described here. In the first column, AG-MP-1M anion exchange resin is packed into a Teflon column (15 cm × 6 mm i.d.). The column is cleaned sequentially with 10 mL 1 M HNO_3 and 5 mL Milli-Q H_2O, and then 10 mL 2 M HCl is used to wash and condition the resin. Subsequently, 2 mL aliquot of the spiked samples are loaded onto the column. Matrix elements (*e.g.*, Na, Mg, Fe, Mn, Zr, Cu, Ni, Pb, In, Mo, Zn *etc.*) are effectively eluted by the decreasing the HCl solution (Table 1). Although partial Sn can be removed with 0.05 M HCl and 0.015 M HCl, respectively, residual Sn together with Cd fractions is eluted with 12 mL 0.0012 M HCl. In the second Bio-Rad column (6 cm × 5 mm i.d.), BPHA extraction resin is packed and cleaned with 5 mL Milli-Q H_2O and then conditioned with 3 mL 1 M HCl. When samples are loaded on the BPHA extraction resin column and the Cd cut is eluted from the resin immediately. Subsequently, another 1.25 mL 1 M HCl can quantitatively elute Cd, whereas the Sn, potential Mo, Zr, and Nb are strongly absorbed in the BPHA extraction resin column. When the Cd solution is evaporated to dryness, ~0.02 mL concentrated HNO_3 is added to dissolve the samples and then ~0.02 mL H_2O_2 is added to decompose the potential organic material. This process is repeated 2 ~ 3 times. After that 2% (m m^{-1}) HNO_3 is added to redissolve Cd samples before Cd isotope measurements.

2.4 ICP-MS determination of elements

During determining the Cd column separation protocol, element mass fractions were determined for all collected aliquots using an Inductively Coupled Plasma Mass Spectrometer (ICP-MS) (Thermo-Scientific XSeries-2) at Tongwei Analytical Technology Co., Ltd (Guiyang). For drift corrections during ICP-MS measurement, Rh, Re, and Bi, as internal references were added to all of the samples. Additionally, a quality control solution (containing Rh, Re, and Bi) as a drift monitor throughout a run was also analyzed repeatedly during ICP-MS measurement. The relative standard deviation (RSD) of elements measured by ICP-MS here was better than 5%.

Table 1 Elution sequence of the two-column procedure

Column procedure	Eluant	Volume (mL)
First column: AG-MP-1M anion exchange resin (2 mL)		
Conditions	2 M HCl	10 (2 mL × 5)
Loading	2 M HCl	2
Matrix removal (Mg, Ca, Ni, Fe, Ga, Ge, Ag, Zr, *etc.*)	2 M HCl	6 (2 mL × 3)
Matrix removal (Mo, In, Pb)	0.2 M HCl	12 (2 mL × 6)
Matrix removal (Zn, Sn, In)	0.05 M HCl	18 (2 mL × 9)
Matrix removal (Sn, In)	0.015 M HCl	6 (2 mL × 3)
Eluting Cd	0.0012 M HCl	12 (2 mL × 6)
Second column: BPHA resin (0.25 mL)		
Conditions	1 M HCl	3 (0.5 mL × 6)
Loading/collecting Cd	1 M HCl	0.2
Collecting Cd	1 M HCl	1.25 (0.25 mL × 5)

Table 2 Thermal Neptune MC-ICP-MS operating conditions

Rf power	1223 W (optimized daily)						
Auxiliary gas (Ar) flow rate	0.89 L min^{-1} (optimized daily)						
Sample gas (Ar) flow rate	0.504 L min^{-1} (optimized daily)						
Cooling gas (Ar) flow rate	15.50 L min^{-1}						
Measurement mode	Static						
Interface cones	H sample cone + X skimmer cone (nickel)						
Acceleration voltage	10 kV						
Detection system	Faraday cups						
Amplifier	10^{11} Ω						
Idle time	3.000 s						
Integration time	4.194 s						
Mass resolution	~400 (low)						
Spray chamber	Dual cyclonic-Scott (quartz)						
Cd sensitivity	360–440 V ppm^{-1} (low-resolution)						
Sample uptake	100 μL min^{-1}						
Cup configuration	L3	L2	L1	C	H1	H3	H4
	^{110}Cd	^{111}Cd	112Cd	^{113}Cd	^{114}Cd	^{116}Cd	^{119}Sn

2.5 Analysis of Cd isotopes

In general, selecting the isotopes used in double spike for isotopic analyses is related to two important criteria. The selected isotopes not only ought to have low abundances relative to the other isotopes of an element present in the DS to conclude the measurement uncertainty but also be free of isobaric or polyatomic interference.[47–49] In light of previous studies,[32,36,49] the DS ^{111}Cd–^{113}Cd was employed to correct the potential isotopic fractionation of Cd during chemical purification as well as mass spectrometry in our study. Importantly, the theoretical calculation[48] and experiment[49] both confirm that the proportion of DS in a mixture can impact analytical precision, and a reasonable range of the proportion of DS in a mixture (or the proportion for a DS and a sample) is important for high precision measurement. In light of the theoretical simulation method,[48] the optimal range of DS proportions in a mixture for high-precise Cd isotopes analyses was determined from 0.3 to 0.7 (*i.e.*, $Cd_{spike}/(Cd_{spike} + Cd_{sample}) = 0.3–0.7$).[49]

Cadmium isotope composition is measured using a Neptune MC-ICP-MS at the Hebei Key Laboratory of Strategic Critical Mineral Resources, Hebei GEO University, Shijiazhuang, 050031, China. Cadmium isotopic measurements are conducted under static mode with a low mass resolution (~400). Data are collected by 1 block with 40 measurement cycles and the integration time for the measurement cycle is 4.194 s per cycle.

Sample solutions (in 2% HNO_3) were introduced into the plasma through an Aridus III desolvation system (Teledyne CETAC Technologies Omaha, NE, USA) equipped with a 100 mL min^{-1} PFA nebulizer system. The signal intensity of ^{112}Cd is approximately 1.8–2.1 V on the Neptune MC-ICP-MS with a Cd concentration of 10 ng mL^{-1}. Our sensitivities (360–440 V ppm^{-1} for ^{112}Cd) are slightly lower than the previously published sensitivities of Pallavicini *et al.* (2014)[39] (517 V ppm^{-1} for ^{112}Cd) and Tan *et al.* (2020)[36] (600–680 V ppm^{-1} for ^{112}Cd). After every measurement of the sample, the inlet system of the instrument is cleaned with two separate 2% (m m^{-1}) HNO_3 washes, respectively, until the ^{111}Cd intensity decreases by <0.1 mV. Details of the typical instrumental operating parameters used in this study are summarized in Table 2.

3. Results and discussion

3.1 Effect of P on Cd isotopic measurement

Although many studies have employed TRU Spec resin for further purifying Cd from the residual Sn,[2,31,32,37,40,42,50] TRU Spec resin-derived organic compounds in the Cd cut can compromise and even generate a detriment on Cd isotopic measurement.[41,43] The structure of TRU Spec resin is (24%) octyl phenyl-*N*,*N*-diisobutyl carbamoylphosphine oxide (CMPO) dissolved in (76%) tri-*n*-butyl phosphate (TBP), and both compounds have phosphor bound organic species.[43,51] The potential polyatomic interferents generated from TRU spec resin are likely phosphorous (P) due to only P has a high enough mass to create potential polyatomic compounds (*e.g.* $^{31}P^{40}Ar^{40}Ar$) across the Cd mass range.[43] Furthermore, Friebel *et al.* (2020)[52] also found that the Sn fractions eluted from a two-layered TRU Spec resin (0.12 mL) and the pre-filter resin (0.04 mL) blending column contained up to 250 μg of P. When the resin-derived organic compounds were oxidized using the H_2O_2/HNO_3 or $HClO_4/HNO_3$ solution, H_3PO_4, H_2O, CO_2, and/or residual organic compounds were created, whereas H_3PO_4 can be stable in the beaker.[41]

To evaluate the potential interference of P, the NIST 3108 Cd standard is doped with P for obtaining different P to Cd concentration ratios and then analyzed for their Cd isotope composition. We find progressive Cd isotopic shifts towards increasingly positive values with the increase of the concentration ratios of [P/Cd], and the undoped bracketing standard shows good external reproducibility with expected values (Fig. 1). Additionally, with the increase of the concentration ratios of [P/Cd] (from 100 to 5000), the corresponding instrumental sensitivity for Cd decreased (from 8% to 50%) compared to the Cd sensitivity of the adjacent unprocessed bracketing standard. Importantly, the isotopic positive shifts and the decrease of instrumental sensitivity in the doped NIST 3108 standard follow the same trend as the experimental observation by Murphy *et al.* (2015).[41] Murphy *et al.* (2015)[41] also found that accurate Cd isotope data were yielded after the Cd cut (collected from 0.2 mL TRU. Spec. resin) was directly extracted with *n*-heptane to remove resin-derived phosphorous organic compounds. However, when the Cd cut was refluxed in concentrated HNO_3 following *n*-heptane extraction chromatography, heavier $\delta^{114/110}Cd$ values were also observed.[41] This may be likely explained by that resin-derived phosphorous organic compounds have been oxidized to H_3PO_4 by the refluxed concentrated HNO_3 and the product of H_3PO_4 cannot be extracted, which therefore interferes the Cd isotope determination.

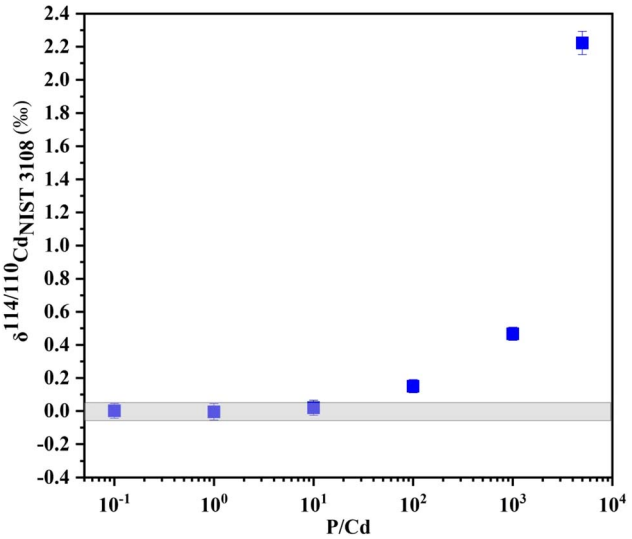

Fig. 1 Plot showing the effect of P doping on measured $\delta^{114/110}Cd_{NIST\ 3108}$ values.

In this study, mass scans of the P solution demonstrate no interfering ion beams across the Cd mass range (masses 106 to 116) indicating that the above-described anomalous shifts in the $\delta^{114/110}Cd$ values of the NIST 3108 standard may be not caused by P-related polyatomic compounds ions but the matrix effect. Similar mass scan results of the concentrated TRU Spec resin column blank have also been shown by Gault-Ringold and Stirling (2012).[43] These results strongly demonstrate that when H_3PO_4, obtained by the oxidation of resin-derived phosphorous organic compounds, forms a enough large ratio of [P/Cd] (*e.g.*, ≥100), it will produce matrix interference on Cd isotopic measurement and result in an increasingly positive Cd isotope shift of samples (Fig. 1). Although resin-derived phosphorous organic compounds can be removed by liquid–liquid extraction with *n*-heptane[41] or using an additional clean-up column containing the pre-filter resin,[52] these methods enlarge the column running time, may decrease the recovery and increase the blank levels for Cd.

3.2 Optimization of the Cd chemical procedure

As shown in Fig. 2a, most of the matrix elements such as Ca, Mg, K, Ti, Fe, Mn, Ni, Cu, Zn, Ga, Ge, Ag, Zr, Mo, In, and Nb can be efficiently removed using the AG-MP-1M resin column. However, the residual Sn fraction is also eluted with Cd (Fig. 2a). In an HCl medium, Cd and Sn may form steadily chloride complex ions $CdCl_4^{2-}$ and $SnCl_6^{2-}$ with relatively similar distribution factors, respectively, and thus $CdCl_4^{2-}$ and $SnCl_6^{2-}$ exhibit relatively similar adsorbability on the AG-MP-1M anion exchange resin. This may mainly explain the incomplete separation between Cd and Sn in AG-MP-1M anion exchange resin.

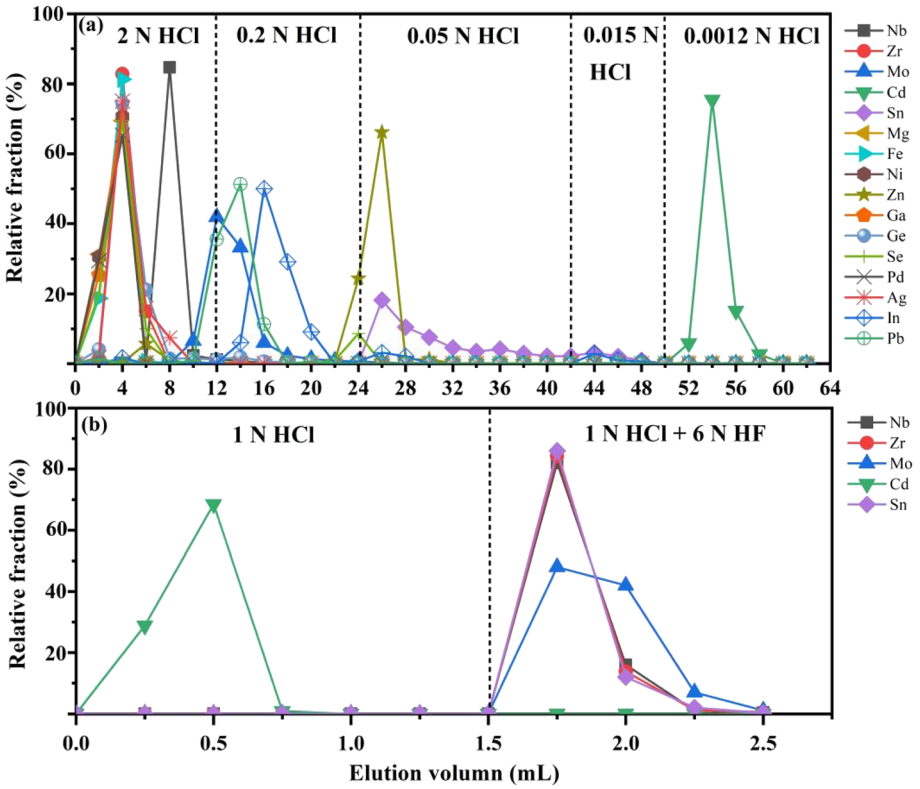

Fig. 2 Elution curves of the Cd separation procedure, (a) the first column with 2 mL AG-MP-1M anion exchange resin and (b) the second column with 0.25 mL BPHA resin.

As discussed in Section 3.1, applying TRU Spec resin has the potential risk of serious interference with Cd isotope measurements. In this study, the BPHA extraction resin instead of TRU Spec resin is employed to further purify Cd after separation of Cd from AG MP-1 anion exchange resin. The BPHA extraction resin is made of *N*-benzoyl-*N*-phenylhydroxylamine (BPHA) impregnated into a microporous acrylic ester polymeric resin (CG-71) without phosphorous organic compounds.[46] This resin exhibits highly selective adsorption for Sn, Mo, Zr, Nb, Hf, Ta, Ti and W (known as fluoride soluble elements), and has the potential for purifying Cd from interference elements such as Sn, Mo, Zr, and Nb.[46,53,54]

We utilize a synthetic solution (Nb : Zr : Mo : Cd : Sn = 1 : 1 : 2 : 5 : 20) to evaluate the separation efficiency of Cd from the interference of Sn, Zr, Nb, and Mo using the BPHA extraction resin. As shown in Fig. 2b, Cd can be directly eluted from the BPHA extraction resin column with 1 M HCl loading solution and subsequent cleaning solution. In contrast, Nb, Sn, Zr, and Mo in 1 M HCl can be strongly adsorbed on the BPHA extraction resin column and then can be removed using 1 M HCl + 6 M HF (Fig. 2b). This indicates that BPHA extraction resin is suitable for Cd purification from the residual Sn and also for potential interference of oxides from Mo, Zr, and Nb.

The procedural blank of Cd may be derived from several steps including digestion, chemical purification, and dissolution for Cd isotope measurement. The total procedural blank of Cd is determined by isotope dilution mass spectrometry here and is generally 0.06 ± 0.02 ng (2SD, $n = 5$), which is approximately 0.2% of the lowest sample size (Cd = 30 ng) for chemical purification, generating negligible influence on Cd isotopic measurement.

3.3 Evaluation of matrix, molecular and isobaric interference

Based on previous studies, precise and accurate Cd isotopic determination is essential to separate Cd from matrix elements completely.[2,30,35–39] To evaluate the purification effectiveness of our presented protocol here, six reference materials (GSP-2, AGV-2, BCR-2, BHVO-2, NOD-P-1, and COQ-1) are purified by our proposed procedure (Table 1). The purification effectiveness of the Cd cut is directly evaluated by measuring the remnant elements in the Cd cut of these six samples. The concentration ratio of [X]/[Cd] (where X denotes a matrix element) is the matrix element to the Cd. The results displayed that except for the P/Cd ratio, Cd is quantitatively purified from matrix elements with the matrix element/Cd ratio being <0.02% (Fig. 3). In our purified samples, matrix elements such as Mg, Ca, Fe, Ni, and Pb have matrix element/Cd ratios lower than 0.0002, which are much lower than the concentration ratio that might produce matrix interference as observed in the doping experiment of Gault-Ringold and Stirling (2012),[43] Liu *et al.* (2019),[35] Tan *et al.* (2020)[36] and Guo *et al.* (2022).[50] This observation demonstrates that the potential matrix effects caused by matrix elements such as Mg, Ca, Fe, Ni, and Pb are negligible for the sample after column separation.

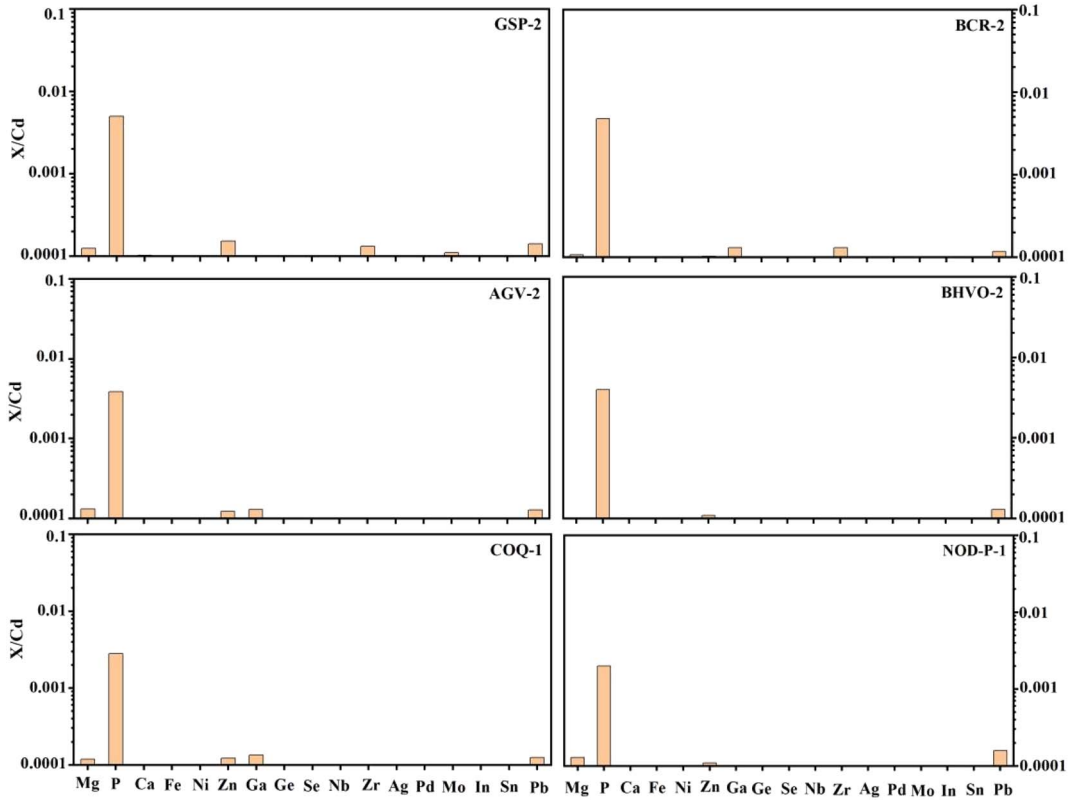

Fig. 3 Purification effectiveness of protocols in removing matrix elements for six selected samples. X denotes a matrix element, and X/Cd is the concentration ratio of matrix elements to Cd.

Table 3 Isobaric and molecular interfering ions for Cd isotopic measurements[a]

Mass/abundances	Molecular interference	Isobaric interference
^{106}Cd (1.25%)	$^{66}Zn^{40}Ar^+$, $^{90}Zr^{16}O^+$	
^{108}Cd (0.89%)	$^{68}Zn^{40}Ar^+$, $^{92}Zr^{16}O^+$, $^{92}Mo^{16}O^+$	^{108}Pd
^{110}Cd (12.5%)	$^{70}Zn^{40}Ar^+$, $^{70}Ge^{40}Ar^+$, $^{94}Zr^{16}O^+$, $^{94}Mo^{16}O^+$, $^{92}Mo^{18}O^+$, $^{109}Ag^1H^+$, $^{93}Nb^{17}O^+$	^{110}Pd
^{111}Cd (12.8%)	$^{71}Ga^{40}Ar^+$, $^{95}Mo^{16}O^+$, $^{97}Mo^{14}N^+$, $^{93}Nb^{18}O^+$	
^{112}Cd (24.1%)	$^{72}Ge^{40}Ar^+$, $^{96}Zr^{16}O^+$, $^{96}Mo^{16}O^+$, $^{96}Ru^{16}O^+$, $^{98}Mo^{14}N^+$, $^{76}Se^{36}Ar^+$	^{112}Sn
^{113}Cd (12.2%)	$^{73}Ge^{40}Ar^+$, $^{97}Mo^{16}O^+$, $^{99}Ru^{14}N^+$, $^{77}Se^{36}Ar^+$	^{113}In
^{114}Cd (28.7%)	$^{74}Ge^{40}Ar^+$, $^{98}Mo^{16}O^+$, $^{98}Ru^{16}O^+$, $^{100}Ru^{14}N^+$, $^{100}Mo^{14}N^+$, $^{77}Se^{36}Ar^+$, $^{74}Se^{40}Ar^+$	^{114}Sn
^{116}Cd (7.49%)	$^{76}Ge^{40}Ar^+$, $^{100}Mo^{16}O^+$, $^{100}Ru^{16}O^+$, $^{76}Se^{40}Ar^+$, $^{80}Se^{36}Ar^+$	^{116}Sn

[a] From the literature of Wombacher *et al.* (2003)[2] and Guo *et al.* (2022).[50]

As shown in Table 3, besides matrix interference, the potential molecular interference on Cd isotopic measurements is related to the formation of molecular interferents such as $ZnAr^+$, $GaAr^+$, $GeAr^+$, ZrO^+, MoO^+, AgH^+, RuO^+, NbO^+, and $SeAr^+$ for Cd isotopes. The concentration ratios of Zn/Cd, Ga/Cd, Ge/Cd, Zr/Cd, Mo/Cd, Ag/Cd, Nb/Cd as well as Se/Cd in our purified samples are lower than 0.000152, 0.000134, 0.000006, 0.000132, 0.000101, 0.000082, 0.000083 and 0.00005, respectively (Fig. 3), which are less than the ratios that could cause measurable Cd isotopic shifts compared with previous studies.[2,30,34–37,50] The Ru content in most terrestrial samples is very low, and no signal for Ru is detected in our measurement of ICP-MS, and thus the potential interference from $Ru^{16}O^+$ (hydro)oxides on Cd isotopic measurement is also negligible. Additionally, the concentration ratios of [P/Cd] are lower than 0.01 and the effect of P on Cd isotopic measurement can also be negligible (Fig. 1 and 3).

Isobaric interference from Pd, In and Sn can induce significant Cd isotopic shifts on Cd isotopic measurements (Table 3). The concentration ratios of Pd/Cd, Sn/Cd, and In/Cd are reduced to <0.000006, <0.0001, and <0.000003, respectively in our purified samples (Fig. 3), which are lower than the ratios that could cause measurable Cd isotopic shifts compared with previous studies.[35–37,50,55] Thus, the potential isobaric interference of Sn, Pd, and In on Cd isotope measurement is also negligible in our study. In brief, the purity of the Cd fractions is suitable for highly precise Cd isotope determination according to the results (Fig. 2 and 3).

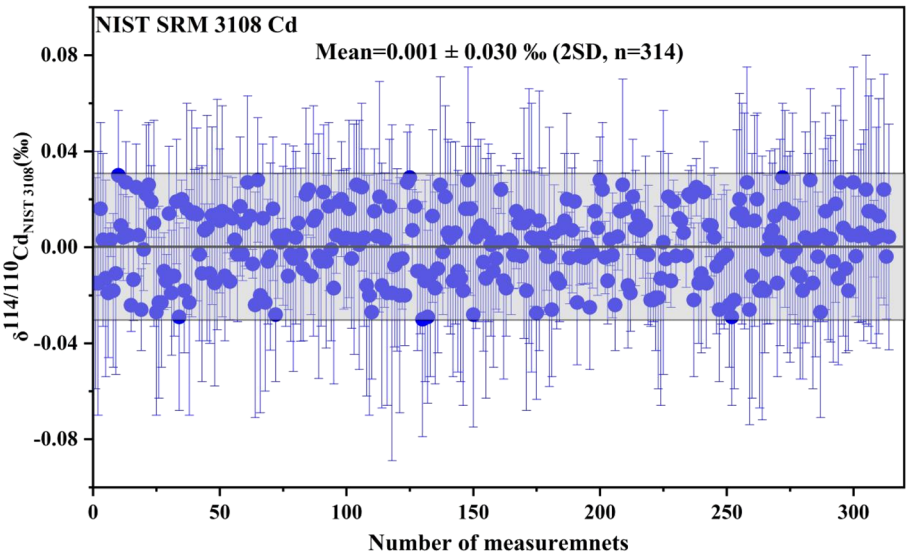

Fig. 4 The long-term reproducibility of $\delta^{114/110}$Cd values for NIST SRM 3108 over seven months. Error bars represent 2 standard errors of each measurement. The grey area represents twice the standard deviation of the $\delta^{114/110}$Cd value of NIST SRM 3108.

3.4 Precision and accuracy

The stability of instrumental measurement is evaluated by repeated analyses of Cd standard solutions (NIST SRM 3108, Spex Cd, and BAM-I012). The long-term analysis of NIST SRM 3018 over seven months obtained an average $\delta^{114/110}$Cd of 0.001 ± 0.030‰ (2SD, $n = 314$) (Fig. 4). Additionally, two Cd standard solutions (Spex Cd and BAM-I012) are used as the secondary reference materials for monitoring the stability during instrumental measurement. Repeated measurements of Spex Cd give the $\delta^{114/110}$Cd value of −2.094 ± 0.049‰ (2SD, $n = 16$) (Fig. 5a) that is indistinguishable from the results of −2.13 ± 0.09‰ (2SD, $n = 74$) and −2.121 ± 0.042‰ (2SD, $n = 18$) reported by Li *et al.* (2018)[34] and Tan *et al.* (2020),[36] respectively. The reported BAM-I012 ranged from −1.251 ± 0.035‰[56] to −1.378 ± 0.110‰,[40] and our measured BAM-I012 yielded a $\delta^{114/110}$Cd value of −1.288 ± 0.056‰ (2SD, $n = 16$) (Fig. 5b), which is in good agreement within uncertainty with the results reported by previous studies.[14,30,31,34–36,40,42,57,58] In light of the above data, the long-term external reproducibility of Cd standard solutions

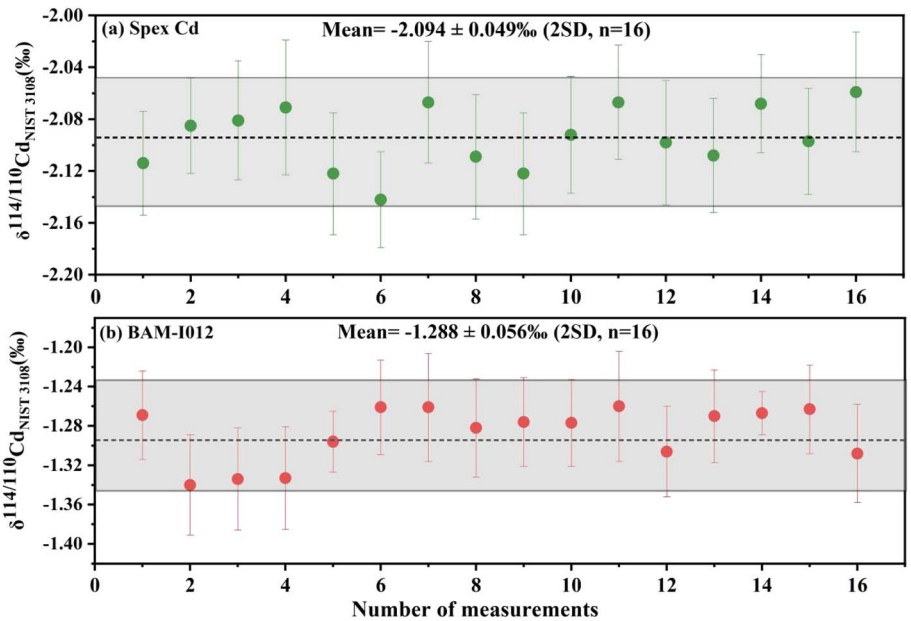

Fig. 5 Reproducibility of $\delta^{114/110}$Cd for long-term measurements of the standard solution Spec-Cd (a) and BAM-I012 (b). Error bars represent 2 standard errors of each measurement. The horizontal line represents the mean $\delta^{114/110}$Cd value. The grey area represents twice the standard deviation of the $\delta^{114/110}$Cd value of Spec-Cd and BAM-I012.

Table 4 Cd isotopic composition of reference materials compared to those previously published[a]

Sample name	Sample type	Cd (μg g^{-1})	Reference	$\delta^{114/110}$Cd	2SD	n
BAM-I012	Reference solution		**This study**	**−1.288**	**0.056**	**16**
			Ripperger and Rehkämper, (2007)[40,c]	−1.378	0.110	
			Shiel *et al.* (2009)[56,c]	−1.251	0.035	
			Schmitt *et al.* (2009)[31,c]	−1.313	0.013	
			Horner *et al.* (2011)[59,c]	−1.296	0.090	
			Abouchami *et al.* (2013)[58]	−1.332	0.040	
			Gault-Ringold *et al.* (2012)[43]	−1.36	0.14	
			Xue *et al.* (2012)[32,c]	−1.329	0.080	
			Gao *et al.* (2013)[22,c]	−1.26	0.10	
			Lambelet *et al.* (2013)[57]	−1.33	0.10	
			Fouskas *et al.* (2018)[42]	−1.34	0.15	
			Li *et al.* (2018)[34]	−1.31	0.09	
			Liu *et al.* (2019)[35]	−1.325	0.043	
			Tan *et al.* (2020)[36]	−1.329	0.045	
Spex Cd	Reference solution		**This study**	**−2.094**	**0.049**	**16**
			Li *et al.* (2018)[34]	−2.130	0.090	
			Tan *et al.* (2020)[36]	−2.121	0.042	
NODP-1	Manganese nodule	22.41	**This study (M = 8)[d]**	**0.196**	**0.073**	**8**
			Cloquet *et al.* (2005)[30,c] (M = 1)	0.04	0.12	1
			Schmitt *et al.* (2009)[31,c] (M = 1)	0.17	0.08	2
			Horner *et al.* (2010)[15,c] (M = 1)	0.20	0.06[b]	3
			Pallavicini *et al.* (2014)[39] (M = 1)	0.120	0.038	4
			Zhang *et al.* (2018)[16] (M = 1)	0.09	0.05	6
			Li *et al.* (2018) (DS)[34] (M = 1)	0.21	0.03	1
			Li *et al.* (2018) (SSB)[34] (M = 1)	0.16	0.08	4
			Liu *et al.*, (2019)[35] (M = 2)	0.163	0.040	8
			Tan *et al.* (2020)[36] (M = 5)	0.133	0.038	23
			Peng *et al.* (2021)[37] (M = 1)	0.12	0.04	4
			Borovicka *et al.* (2021)[60] (M = 5)	0.14	0.07	5
			Lu *et al.* (2021)[61] (M = 2)	0.135	0.074	4
			Gou *et al.* (2022)[50] (M = 1)	0.16	0.04	8
NOD-A-1	Manganese nodule	18.97	**This study (M = 3)[d]**	**0.193**	**0.047**	**3**
			Cloquet *et al.* (2005)[30,c] (M = 1)	−0.16	0.12	1
			Schmitt *et al.* (2009)[31,c] (M = 2)	0.13	0.02	2
			Horner *et al.* (2010)[15,c] (M = 1)	0.23	0.06[b]	2
			Pallavicini *et al.* (2014)[39] (M = 2)	0.086	0.031	4
			Murphy *et al.* (2015)[41] (M = 2)	0.17	0.05	2
			Zhang *et al.* (2018)[16] (M = 2)	0.04	0.06	6
			Li *et al.* (2018)[34] (M = 1)	0.16	0.10	4
			Tan *et al.* (2020)[36] (M = 3)	0.124	0.067	14
			Peng *et al.* (2021)[37] (M = 1)	0.08	0.02	4
			Borovicka *et al.* (2021)[60] (M = 5)	0.12	0.01	5
BCR-2	Basalt	0.202	**This study (M = 3)[d]**	**0.026**	**0.037**	**3**
			Liu *et al.*, (2019)[35] (M = 4)	0.018	0.067	14
			Tan *et al.* (2020)[36] (M = 2)	−0.030	0.063	4
			Lu *et al.* (2021)[61] (M = 2)	0.008	0.074	6
BHVO-2	Basalt	0.091	**This study (M = 3)[d]**	**−0.014**	**0.061**	**3**
			Liu *et al.*, (2019)[35] (M = 2)	0.039	0.047	8
			Tan *et al.* (2020)[36] (M = 2)	−0.031	0.077	4
			Lu *et al.* (2021)[61] (M = 2)	0.021	0.074	6
GSP-2	Granodiorite	0.093	**This study (M = 3)[d]**	**−0.228**	**0.079**	**3**
			Liu *et al.*, (2019)[35] (M = 2)	−0.196	0.068	7
COQ-1	Carbonatite	0.611	**This study (M = 3)[d]**	**0.123**	**0.048**	**3**
			Liu *et al.*, (2019)[35] (M = 4)	0.098	0.052	8
AGV-2	Andesite	0.069	**This study (M = 3)[d]**	**0.081**	**0.083**	**3**
			Wiggenhauser *et al.* (2016)[62] (M = 1)	0.11	0.11	2
			Palk *et al.* (2018)[63] (M = 1)	0.15	0.08	1
			Liu *et al.*, (2019)[35] (M = 4)	0.090	0.035	8

[a] n-The number of measurements. M – the number of independent digestions of the same reference material powder. 2SD = 2 times the standard deviation of n repeated measurements. [b] The uncertainties are quoted as two standard errors (2 SE) and represent the within-run precision of each Cd isotope measurement. [c] The $\delta^{114/110}$Cd value of samples in previous studies was recalculated relative to NIST SRM 3108, according to Abouchami *et al.* (2013).[58] [d] The averaged $\delta^{114/110}$Cd value of every geological material is reported with calculated means ± 2SD (in bold).

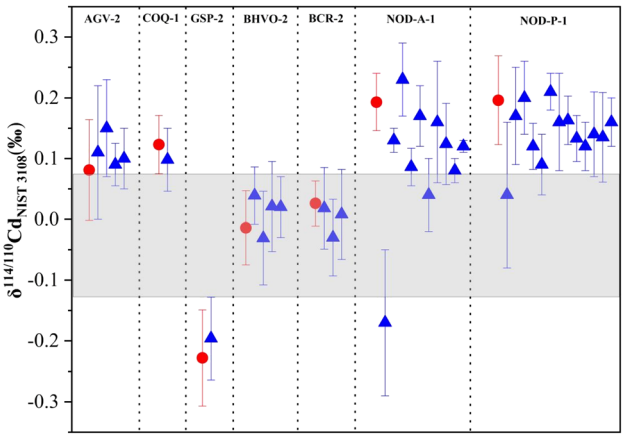

Fig. 6 $\delta^{114/110}$Cd values of geological reference materials including the data from this study and previous studies. Red circles represent the data from this study; blue triangle symbols represent the literature data.[14,16,30,34–37,39,41,50,60–63] Error bars reflect two standard deviations (2SD). The grey area represents the $\delta^{114/110}$Cd value of Bulk Silicate Earth (−0.03 ± 0.10‰; Schmitt *et al.*, 2009).

(NIST SRM 3108, Spex Cd, and BAM-I012) is better than ± 0.056‰ (2SD, $n = 346$).

To estimate the long-term external precision of real samples, reference materials NOD-P-1 are repeatedly subjected to the full procedure including digestion, separation, and isotopic measurements. In these repeated experiments, we not only obtained identical Cd isotopic results within the uncertainty of NOD-P-1 compared with the reported data but also achieved the analytical precision of 0.196 ± 0.073‰ (2SD, $n = 8$) for NOD-P-1 samples in 2022 (Table 4). This analytical precision can distinguish the fractionation of Cd isotopes in various geochemical processes in nature.

4. Cadmium isotope compositions of soil and sediment reference materials

Cd isotopic compositions measured in the seven reference materials are reported in Table 4 and illustrated in Fig. 6. Based on the work summarized by Abouchami *et al.* (2013),[58] all the Cd isotopic data quoted from the literature here are re-normalized relative to NIST SRM 3108 Cd together with the $\delta^{114/110}$Cd notation. The conversion formula for the Cd isotopic data is provided by the following equation:[58] $\delta^{114/110}Cd_{X\text{-}NIST\ 3108} = \delta^{114/110}Cd_{X\text{-}A} + \delta^{114/110}Cd_{A\text{-}NIST\ 3108} + (\delta^{114/110}Cd_{X\text{-}A}) \times (\delta^{114/110}Cd_{A\text{-}NIST\ 3108})/1000$, where X and A represent the actual sample and original laboratory standard, respectively.

The reported $\delta^{114/110}$Cd values of manganese nodule NOD-A-1 exhibited significant variation ranging from −0.16 ± 0.12‰[30] to 0.23 ± 0.06‰.[15] Our measured $\delta^{114/110}$Cd value of NOD-A-1 (0.193 ± 0.047‰; 2SD, $n = 3$) is higher than the value reported by Cloquet *et al.* (2005)[30] and Zhang *et al.* (2018),[16] respectively, but is in accord with other reported $\delta^{114/110}$Cd values (Table 4). Furthermore, the Cd mass fractions of NOD-A-1 (18.97 μg g^{-1}) determined by isotope dilution mass spectrometry in this study are also remarkably higher than those reported in previous results (6.13 μg g^{-1} (ref. 36) to 7.60 μg g^{-1}).[60] These differences in the reported $\delta^{114/110}$Cd values and Cd mass fractions for NOD-A-1 may result from the heterogeneity of the sample.

The measured $\delta^{114/110}$Cd values for ferromanganese nodules NOD-P-1, basalt BHVO-2, basalt BCR-2, carbonate COQ-1, andesite AGV-2, and granodiorite GSP-2 are in good agreement within uncertainty with reported values (Table 4).[16,30,31,34–37,39,50,61] Both basalt BHVO-2 and BCR-2 exhibit a similar Cd isotopic composition to the average bulk silicate earth (BSE) (−0.03 ± 0.10‰) proposed by Schmitt *et al.* (2009)[14] (Fig. 6). The carbonate COQ-1 and andesite AGV-2 exhibit a slightly heavier $\delta^{114/110}$Cd value than BSE, whereas granodiorite GSP-2 is enriched in lighter Cd isotopic composition relative to BSE (Fig. 6). The overall variation of $\delta^{114/110}$Cd values of these analyzed igneous rock reference materials is up to 0.351‰, which may suggest Cd isotopic fractionation during high-temperature processes. Limited by the lack of Cd isotope data for igneous rocks, more research should be performed on these questions.

5. Conclusion

We present a new two-stage Cd purification protocol together with a double spike MC-ICP-MS method for routine high-precision Cd isotope analysis. P doping experiments indicate that when the [P/Cd] ratio is ≥100 in the sample, it will result in an increasingly positive Cd isotope shift of samples. This observation strongly indicates that TRU Spec resin-derived phosphorous organic compounds may mainly cause a positive Cd isotope shift. In particular, mass scans of the P solution reveal no interfering ion beams across the Cd mass range (masses 106 to 116). This result further indicates that anomalous shifts in the Cd isotope measurement may be caused by the P-related matrix effect. The BPHA extraction resin exhibits sufficient Cd purification from interference elements especially Sn, Mo, Zr, and Nb. The $\delta^{114/110}$Cd values measured in geological reference materials are in agreement within uncertainty with the reported results, suggesting the precision and accuracy of the proposed method. The Cd isotope compositions of BHVO-2, BCR-2, AGV-2, COQ-1, and GSP-2 exhibit different deviations relative to BSE, demonstrating that high-temperature magmatic evolution processes may generate Cd isotopic fractionation.

Author contributions

Qiao-Hui Zhong performed the experiments. Chun-Hui Zhu and Neng-Ping Shen contributed to the column chemistry. Qiao-Hui Zhong, Lu Yin, Shuang Yan and Zhao-Yang Wang contributed to the MC-ICPMS measurements. Jie Li and Qiao-Hui Zhong analyzed the data. Qiao-Hui Zhong wrote the manuscript (original draft, formal analysis) and Jie Li directed the manuscript (formal analysis, conceptualization, supervision, writing – review, editing, project administration).

Conflicts of interest

There are no conflicts of interest to declare.

Acknowledgements

This research was funded by the National Key Research and Development Project of China (grant number 2020YFA0714801) and was supported by the Guizhou Provincial Science and Technology Project (No. [2020] 3Y003). We are grateful to Prof. Zhu jian-ming at the China University of Geosciences (Beijing) for providing the standard solution of BAM-I012 (Lot: C152382M) and Spex-Cd (Lot: CL8-71CDY). We are grateful to Dr Zhang Le for his help in Cd isotope determination on MC-ICP-MS. The authors also thank Mrs Guan qing-dian, Wang huan, and Leng hui for their assistance with the determination of matrix element concentrations, and Chen da-ming, Wu wen-chang, Yan mao, Wu meng, Luo jiang-lan and Wang zhi-dan for their assistance with the beaker and acid preparation. Finally, we wish to thank two reviewer and editor for their thoughtful and constructive comments. This is contribution No. IS-3323 from GIGCAS.

References

1 W. Pritzkow, S. Wunderli, J. Vogl and G. Fortunato, *Int. J. Mass Spectrom.*, 2007, **261**, 74–85.
2 F. Wombacher, M. Rehkämper, K. Mezger and C. Münker, *Geochim. Cosmochim. Acta*, 2003, **67**, 4639–4654.
3 F. Wombacher, M. Rehkämper, K. Mezger, A. Bischoff and C. Münker, *Geochim. Cosmochim. Acta*, 2008, **72**, 646–667.
4 C. Zhu, H. Wen, Y. Zhang, H. Fan, S. Fu, J. Xu and T. Qin, *Sci. China Earth Sci.*, 2013, **56**, 2056–2065.
5 C. Zhu, H. Wen, Y. Zhang, S. Fu, H. Fan and C. Cloquet, *Miner. Deposita*, 2016, **52**, 675–686.
6 H. J. Wen, C. W. Zhu, Y. X. Zhang, C. Cloquet, H. F. Fan and S. H. Fu, *Sci. Rep.*, 2017, **6**, 25273.
7 T. Wu, Z. Huang, Y. He, M. Yang, H. Fan, C. Wei, L. Ye, Y. Hu, Z. Xiang and C. Lai, *Ore Geol. Rev.*, 2021, **135**, 104214.
8 F. Lacan, R. Francois, Y. Ji and R. M. Sherrell, *Geochim. Cosmochim. Acta*, 2006, **70**, 5104–5118.
9 S. Ripperger, M. Rehkämper, D. Porcelli and A. N. Halliday, *Earth Planet. Sci. Lett.*, 2007, **261**, 670–684.
10 W. Abouchami, S. J. G. Galer, H. J. W. de Baar, R. Middag, D. Vance, Y. Zhao, M. Klunder, K. Mezger, H. Feldmann and M. O. Andreae, *Geochim. Cosmochim. Acta*, 2014, **127**, 348–367.
11 T. M. Conway and S. G. John, *Geochim. Cosmochim. Acta*, 2015, **148**, 269–283.
12 D. J. Janssen, W. Abouchami, S. J. G. Galer and J. T. Cullen, *Earth Planet. Sci. Lett.*, 2017, **472**, 241–252.
13 M. Sieber, T. M. Conway, G. F. de Souza, H. Obata, S. Takano, Y. Sohrin and D. Vance, *Chem. Geol.*, 2019, **511**, 494–509.
14 A.-D. Schmitt, S. J. G. Galer and W. Abouchami, *Earth Planet. Sci. Lett.*, 2009, **277**, 262–272.
15 T. J. Horner, M. Schönbächler, M. Rehkämper, S. G. Nielsen, H. Williams, A. N. Halliday, Z. Xue and J. R. Hein, *Geochem. Geophys. Geosystems*, 2010, 1–10.
16 Y. Zhang, H. Wen, C. Zhu, H. Fan and C. Cloquet, *Chem. Geol.*, 2018, **481**, 110–118.
17 R. Frei, L. Xu, J. A. Frederiksen and B. Lehmann, *Chem. Geol.*, 2021, **563**, 120061.
18 J. A. Frederiksen, R. M. Klaebe, J. Farkas, P. K. Swart and R. Frei, *Sci. Total Environ.*, 2022, **806**, 150565.
19 C. Cloquet, J. Carignan, G. Libourel, T. Sterckeman and E. Perdrix, *Environ. Sci. Technol.*, 2006, **40**, 2525–2530.
20 A. E. Shiel, D. Weis and K. J. Orians, *Sci. Total Environ.*, 2010, **408**, 2357–2368.
21 A. E. Shiel, D. Weis, D. Cossa and K. J. Orians, *Geochim. Cosmochim. Acta*, 2013, **121**, 155–167.
22 B. Gao, H. Zhou, X. Liang and X. Tu, *Environ. Pollut.*, 2013, **181**, 340–343.
23 H. Wen, Y. Zhang, C. Cloquet, C. Zhu, H. Fan and C. Luo, *Appl. Geochem.*, 2015, **52**, 147–154.
24 M. Salmanzadeh, A. Hartland, C. H. Stirling, M. R. Balks, L. A. Schipper, C. Joshi and E. George, *Environ. Sci. Technol.*, 2017, **51**, 7369–7377.
25 M. Imseng, M. Wiggenhauser, A. Keller, M. Muller, M. Rehkamper, K. Murphy, K. Kreissig, E. Frossard, W. Wilcke and M. Bigalke, *Environ. Sci. Technol.*, 2018, **52**, 1919–1928.
26 P. Wang, Z. Li, J. Liu, X. Bi, Y. Ning, S. Yang and X. Yang, *Environ. Pollut.*, 2019, **249**, 208–216.
27 X. Zhang, Y. Yan, S. A. Wadood, Q. Sun and B. Guo, *Appl. Geochem.*, 2020, **123**, 104776.
28 Q. Zhong, M. Yin, Q. Zhang, J. Beiyuan, J. Liu, X. Yang, J. Wang, L. Wang, Y. Jiang, T. Xiao and Z. Zhang, *J. Hazard. Mater.*, 2021, **411**, 125015.
29 K. J. R. Rosman and J. R. de Laeter, *Int. J. Mass Spectrom.*, 1975, **16**, 385–394.
30 C. Cloquet, O. Rouxel, J. Carignan and G. Libourel, *Geostand. Geoanal. Res.*, 2005, **29**, 95–106.
31 A. D. Schmitt, S. J. G. Galer and W. Abouchami, *J. Anal. At. Spectrom.*, 2009, **24**, 1079–1088.
32 Z. Xue, M. Rehkamper, M. Schonbachler, P. J. Statham and B. J. Cole, *Anal. Bioanal. Chem.*, 2012, **402**, 883–893.
33 R. Wei, Q. Guo, H. Wen, J. Yang, M. Peters, C. Zhu, J. Ma, G. Zhu, H. Zhang and L. Tian, *Anal. Methods*, 2015, **7**, 2479–2487.
34 D. Li, M. L. Li, W. R. Liu, Z. Z. Qin and S. A. Liu, *Geostand. Geoanal. Res.*, 2018, **42**, 593–605.
35 M. S. Liu, Q. Zhang, Y. Zhang, Z. Zhao, F. Huang and H. M. Yu, *Geostand. Geoanal. Res.*, 2019, **44**, 169–182.
36 D. Tan, J.-M. Zhu, X. Wang, G. Han, Z. Lu and W. Xu, *J. Anal. At. Spectrom.*, 2020, **35**, 713–727.
37 H. Peng, D. He, R. Guo, X. Liu, N. S. Belshaw, H. Zheng, S. Hu and Z. Zhu, *J. Anal. At. Spectrom.*, 2021, **36**, 390–398.
38 B. Gao, Y. Liu, K. Sun, X. Liang, G. Sheng and J. Fu, *Anal. Chim. Acta*, 2008, **612**, 114–120.
39 N. Pallavicini, E. Engstrom, D. C. Baxter, B. Ohlander, J. Ingri and I. Rodushkin, *J. Anal. At. Spectrom.*, 2014, **29**, 1570–1584.

40 S. Ripperger and M. Rehkämper, *Geochim. Cosmochim. Acta*, 2007, **71**, 631–642.
41 K. Murphy, M. Rehkamper, K. Kreissig, B. Coles and T. van de Flierdt, *J. Anal. At. Spectrom.*, 2016, **31**, 319–327.
42 F. Fouskas, L. Ma, M. A. Engle, L. Ruppert, N. J. Geboy and M. A. Costa, *Appl. Geochem.*, 2018, **96**, 100–112.
43 M. Gault-Ringold and C. H. Stirling, *J. Anal. At. Spectrom.*, 2012, **27**, 449.
44 D. M. Borrok, R. B. Wanty, W. I. Ridley, R. Wolf and P. J. Lamothe, *Chem. Geol.*, 2007, **242**, 400–414.
45 J. Chapman, T. F. D. Mason, D. J. Weiss, B. J. Coles and J. J. Wilkinson, *Geostand. Geoanal. Res.*, 2007, 5–16.
46 J. Li, X.-R. Liang, L.-F. Zhong, X.-C. Wang, Z.-Y. Ren, S.-L. Sun, Z.-F. Zhang and J.-F. Xu, *Geostand. Geoanal. Res.*, 2014, **38**, 345–354.
47 F. Albarede and B. Beard, *Rev. Mineral. Geochem.*, 2004, **55**, 113–152.
48 J. F. Rudge, B. C. Reynolds and B. Bourdon, *Chem. Geol.*, 2009, **265**, 420–431.
49 L. Zhang, J. Li, Y.-G. Xu and Z.-Y. Ren, *J. Anal. At. Spectrom.*, 2018, **33**, 555–562.
50 C. Guo, T. Li, G. Li, T. Chen, L. Li, L. Zhao and J. Ji, *J. Anal. At. Spectrom.*, 2022, **37**, 2470–2479.
51 M. Losno, J. Pelle, M. Marie and I. Ferrante, *Talanta*, 2018, **185**, 586–591.
52 M. Friebel, E. R. Toth, M. A. Fehr and M. Schönbächler, *J. Anal. At. Spectrom.*, 2020, **35**, 273–292.
53 X. J. Yang and C. Pin, *Anal. Chim. Acta*, 2002, **458**, 375–386.
54 S. Sun and J. Li, *Microchem. J.*, 2015, **119**, 102–107.
55 L. E. Wasylenki, J. W. Swihart and S. J. Romaniello, *Geochim. Cosmochim. Acta*, 2014, **140**, 212–226.
56 A. E. Shiel, J. Barling, K. J. Orians and D. Weis, *Anal. Chim. Acta*, 2009, **633**, 29–37.
57 M. Lambelet, M. Rehkämper, T. van de Flierdt, Z. Xue, K. Kreissig, B. Coles, D. Porcelli and P. Andersson, *Earth Planet. Sci. Lett.*, 2013, **361**, 64–73.
58 W. Abouchami, S. J. G. Galer, T. J. Horner, M. Rehkamper, F. Wombacher, Z. Xue, M. Lambelet, M. Gault-Ringold, C. H. Stirling and M. Schonbachler, *Geostand. Geoanal. Res.*, 2013, **37**, 5–17.
59 T. J. Horner, R. E. M. Rickaby and G. M. Henderson, *Earth Planet. Sci. Lett.*, 2011, **312**, 243–253.
60 J. Borovicka, L. Ackerman and J. Rejsek, *Talanta*, 2021, **221**, 121389.
61 Z. Lu, J. M. Zhu, D. Tan, X. Wang and Z. Zheng, *Geostand. Geoanal. Res.*, 2021, **45**, 565–581.
62 M. Wiggenhauser, M. Bigalke, M. Imseng, M. Muller, A. Keller, K. Murphy and K. Kreissig, *Environ. Sci. Technol.*, 2016, **50**, 9223–9231.
63 E. Palk, R. Andreasen, M. Rehkämper, A. Stunt, K. Kreissig, B. Coles, M. Schönbächler and C. Smith, *Meteorit. Planet. Sci.*, 2018, **53**, 167–186.